

18. V. Tzeng and E. E. Kundhart, "New insight into streamer development," Fourth IEEE Pulsed Power Conference, New York (1983).
19. N. S. Rudenko and V. I. Smetanin, "Mechanism of propagation of streamers on the basis of plasma oscillations," *Izv. Vyssh. Uchebn. Zaved., Fiz.*, No. 7 (1977).
20. O. A. Omarov, M. B. Khachalov, et al., "Formation of a spark channel," *Fiz. Plazmy*, 4, No. 2 (1978).
21. L. P. Babich, "Role of plasma waves in the spark breakdown of gases," *Fiz. Plazmy*, 7, No. 6 (1981).
22. V. P. Ginzburg and A. V. Gurevich, "Nonlinear phenomena in plasma in an alternating electric field," *Usp. Fiz. Nauk*, 10, No. 2 (1960).
23. L. P. Babich and Yu. L. Stankevich, "Criterion for the transition from a streamer mechanism of discharge to continuous electron acceleration," *Zh. Tekh. Fiz.*, 42, No. 8 (1972).
24. G. A. Mesyats, Yu. I. Bychkov, and V. V. Kremnev, "Pulsed nanosecond electrical discharge in a gas," *Usp. Fiz. Nauk*, 107, No. 2 (1972).
25. G. V. Gadiyak, K. A. Nasyrov, et al., "Mathematical simulation of gas-discharge lasers," Preprint [in Russian], *Inst. Teor. Prikl. Mekh. Sib. Otd. Akad. Nauk SSSR*, No. 30-85, Novosibirsk (1985).

MODEL OF A STREAMER IN A LONG DISCHARGE GAP

V. P. Meleshko and V. A. Shveigert

UDC 537.521

Detailed experimental data have been published on the development of a streamer with characteristic times substantially longer than the avalanche-streamer transition (AST) time. The results of the different experiments are not completely consistent even at the qualitative level. Rudenko and Smetanin [1] and Davidenko et al. [2], observing that a streamer formed at the center of a discharge gap and propagated toward the electrodes, determined that the velocity of both ends of the streamer increases rapidly and continuously. Bayle et al. [3] found that the streamer velocity became saturated as the channel moved through a long discharge gap. The contradiction is not resolved by the results of other experimental studies. Kline [4], Reininghaus [5], and Dhali and Williams [6] carried out calculations of a streamer in the diffusion-drift approximation. However, they studied only the initial stage in the formation of the streamer channel, which does not indicate the nature of the channel development in a long discharge gap at long characteristic times. The development of a long streamer is described only phenomenologically by existing models [7, 8].

In this study, in the diffusion-drift approximation we numerically simulate the development of a streamer in neon under one-electrode initiation of a discharge at the center of the gap with the gas at atmospheric pressure. The gap was assumed to be unbounded and the effect of the electrodes was not taken into account. The streamer channel was calculated to grow to a length of up to 7 cm. Two phases were shown to exist in the development of the streamer: an acceleration phase, when the velocity of the streamer increases rapidly; and a phase of quasi-steady development, in which case the streamer velocity changes very slowly.

The two-dimensional calculation of streamer development over a long time requires much computer time. Accordingly, a one-dimensional model is used to calculate the transport of charged particles. The initial stage of streamer development has already been calculated in such a model [4].

The behavior of electrons and ions is described by the equations

$$\frac{\partial n_e}{\partial t} + \mu_e \frac{\partial n_e E}{\partial x} = D_e \frac{\partial^2 n_e}{\partial x^2} + \alpha n_e \mu_e E - \beta n_e n_i + \frac{n^*}{\tau_{ac}},$$

$$\frac{\partial n_i}{\partial t} = \alpha n_e \mu_e E - \beta n_e n_i + \frac{n^*}{\tau_{ac}},$$

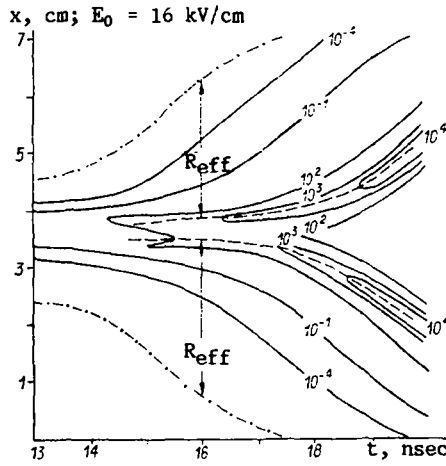


Fig. 1

where n_e and n_i are the electron and ion densities, n^* is the density of excited atoms, E is the electric field in the gap, μ_e is the electron mobility, D_e is the electron diffusion coefficient, $1/\tau_{ac} = \langle \sigma_{ac} v_a \rangle n_a$, v_a is the thermal velocity of the gas atoms, n_a is the gas-atom density, β is the recombination coefficient, α is the coefficient of collision ionization, and σ_{ac} is the cross section for associative ionization.

The electric field is calculated by using the model of disks [5]

$$E(x) = E_0 + 2\pi e \int [n_i(x') - n_e(x')] \left\{ \frac{x-x'}{|x-x'|} - \frac{x-x'}{\sqrt{R_c^2 + (x-x')^2}} \right\} dx'$$

Here E_0 is the external electric field, e is the elementary charge, and R_c is the radius of the streamer channel. Associative ionization is considered as the secondary mechanism of ionization. The mechanism of excitation of the gas under interaction with resonance radiation, excitation of the gas atoms by electrons, and spontaneous de-excitation of these atoms are taken into account. Radiation transfer is assumed to occur at the effective resonance level. The mechanism of broadening of the radiation line has been considered. The distribution of the excited atoms is described by the Biberman-Holstein equation

$$\frac{\partial n^*(x)}{\partial t} = \frac{n_e(x)}{\tau_{ex}} - \frac{n^*(x)}{\tau_l} - \frac{n^*(x)}{\tau_{ac}} + \frac{1}{\tau_l} \int n^*(x') G(x, x') dx'$$

The kernel $G(x, x')$ represents the probability that radiation from a point with coordinate x is absorbed in an elementary volume V at point x' . In the calculations carried out the relation $h \ll \lambda_p^0$ (λ_p^0 is the mean free path of a photon at the center of the line) was always satisfied for the grid spacing h . The broadening mechanism was assumed to be Lorentzian.

The simple analytical relation $G(x, x') = \sqrt{\lambda_p^0} V / (\sqrt{\pi} R^{7/2})$ [9], was used for $G(x, x')$ and the coefficient collision excitation was $\tau_{ex} = \delta \alpha \mu_e E$ (δ is the number of excitation events per collision ionization event and τ_l is the lifetime of the effective resonance level).

From the results of two-dimensional simulation of a streamer [6, 10] we can conclude that the transverse dimension of the streamer channel varies very little from time when AST occurs. The channel radius R_c , therefore, was assumed to be constant and equal to the diffusion radius of the avalanche up until AST took place. Comparison of test calculations of AST in nitrogen with the data of [11] showed that AST is described fairly well by the model adopted.

An avalanche is known to multiply in accordance with Townsend's law $N_e \sim \exp(\alpha v_e t)$ until the number of electrons in it is $N_e \sim 10^5$ [12]. The calculation was started with $N_e = 10^5$ and time $t_{av} = \ln(N_e) / \alpha \mu_e E_0$.

The electron density in the initial avalanche was assigned a Gaussian distribution along

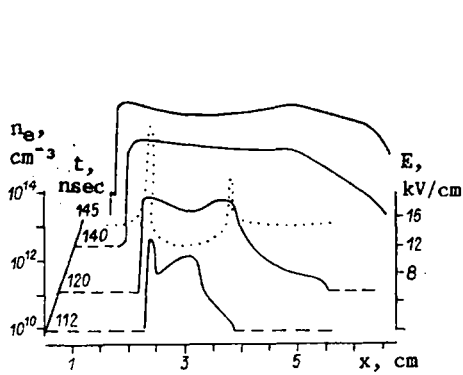


Fig. 2

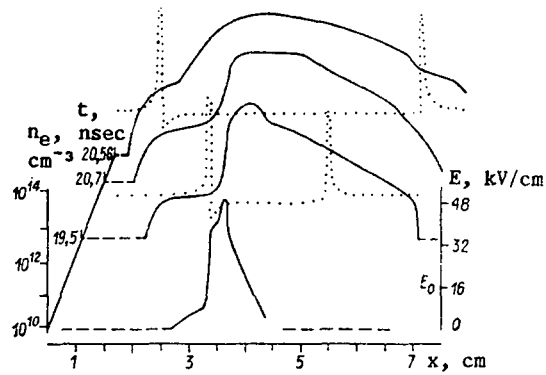


Fig. 3

the axis of the streamer channel with a characteristic avalanche size $R \sim \sqrt{4D_e t_{av}}$. The gas parameters were taken from [13]: $\mu_e = 800 \text{ cm}^2/\text{V}\cdot\text{sec}$, $D_e = 7 \cdot 10^3 \text{ cm}^2/\text{sec}$, $\alpha/p = A \exp[-B/(E/p)]$, $\beta = 0$, $A = 9.98 \cdot 10^3 \text{ cm}^{-1}\cdot\text{Pa}^{-1}$, and $B = 2.7 \cdot 10^4 \text{ V/cm}\cdot\text{Pa}$. The literature does not give the necessary information about the kinetic parameters τ_{ac} and τ_{av} of neon. Kanl and Seyfried [14] chose some levels, which are capable of participating in the transfer of excitation with subsequent associative ionization and introduced complex kinetic parameters for them. In the present study the parameters of secondary ionization are typical of neon resonance levels which are capable of participating in this process ($\tau_{\lambda} = 10^{-8} \text{ sec}$, $\tau_{ac} = 5 \cdot 10^{-8} \text{ sec}$, $\delta = 10$ [9, 14, 15]). The indeterminacy in the choice of the indicated parameters and the broadening mechanism has only a weak effect on the nature of the streamer development. In the given case, e.g., a quasirandom mechanism operates at the edges of the lines. This aspect is not fundamental, however, for the problem under consideration. Various aspects of secondary ionization are discussed in detail below.

The calculation was carried out in the Lagrangian coordinate system on a uniform moving grid with condensations in the region of strong electric-field gradients. In order to reduce the effect of numerical diffusion, the development of secondary avalanches, formed in the gap far from the streamer channel, was calculated separately by the particle method with subsequent interpolation to the grid. The minimum grid spacing along the x axis was $h_{min} = 0.2 R_c$. Two limitations were taken into account when choosing the time interval: Courant stability for an explicit scheme approximating the transfer equation $\tau_c = \min_i \{1/(v_i/h_i + 2D_e/h_i^2)\}$ (h_i and v_i are the size of the i-th cell and the drift velocity of electrons in it); the characteristic charge relaxation time in the plasma is $\tau_r = 1/(4\pi\sigma)$ (σ is the plasma conductivity). The time interval should not exceed τ_r . Hence $\tau = \min[\tau_c, \tau_r]$. As the avalanche development begins $\tau_c < \tau_r$. Up until AST occurs the channel conductivity increases and $\tau_c \lesssim \tau_r$. With the development of the streamer after AST the conductivity of the plasma in the channel decreases so much that $\tau_r \ll \tau_c$. In trial calculations after AST we assumed that $\tau = \tau_r$. With this interval in the case of long times, a numerical instability nevertheless arose and, therefore, in the stage of a developed streamer the calculations were done with $\tau = 0.2 \tau_r$. A further reduction of τ did not lead to any appreciable changes in the results of the calculations.

The AST mechanism has been studied fairly well [11, 16] and, therefore, we shall not focus attention on it. By the time AST occurs a characteristic electric-field distribution with two maxima at the ends is formed in the channel. The field inside the channel is $(0.6-0.8)E_0$ and varies only slightly. Then a linear distribution of charge is established in the streamer channel. All times are measured from the time when an initiating electron appears in the gap. Figure 1 shows the graph of the luminosity isolines of the streamer channel, which was obtained for $E_0 = 16 \text{ kV/cm}$. In this figure and in subsequent figures the x axis is directed opposite to the external electric field. Marked on the isolines are the corresponding relative levels of luminosity, which were determined from the density n^* of excited atoms at the given point in the channel. The dashed-dotted lines represent the boundary of the region where secondary ionization is induced by the radiation of the channel. The effect of this region on the development of the streamer is discussed below. The dashed lines indicate the positions of the maximum of the electric field at the ends of the channel. We see that during the streamer development the velocity of propagation of the leading edge of the

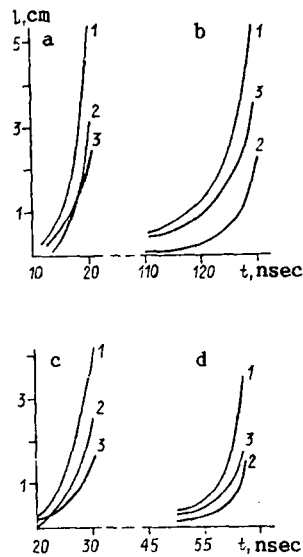


Fig. 4

luminosity increases abruptly. The slope of all the brightest lines then increases. Unless stipulated otherwise, here and below we deal with both anode and cathode streamers. Intensive ionization corresponds to a rapid increase in the channel luminosity. The development of an avalanche in a weak external field ($E_0 \lesssim 9$ kV/cm) has a superexponential segment, i.e., an interval of time when the number of electrons in the avalanche varies more rapidly than according to the law $N_e \sim \exp(\alpha v_e t)$. In relatively strong external fields ($E_0 \geq 16$ kV/cm) the electron multiplication is always slower than exponential. Figures 2 and 3 show the electron-density distributions in the gap at different times for $E_0 = 8.6$ and 16 kV/cm, respectively. The dashed line indicates the existence of a region of weakly ionized gas ($n_e \lesssim 10^6$ cm $^{-3}$) on either side of the streamer channel because of secondary ionization. The scale of densities n_e is laid off along the left vertical axis and the scale of the electric field strength is laid off along the right vertical axis. The field distributions in the gap are indicated by points in Figs. 2 and 3 but not for all times so as not to overload the drawing.

After the AST a long precursor is formed ahead of the channel (Fig. 3). Then a fast ionization wave moves along the precursor toward the cathode. The rate at which the maximum of the field at the cathode end of the channel is displaced increases sharply in this case. The development of the streamer in the direction of the anode is more even, but its rate increases. At the time of an abrupt increase in the velocities of the streamers the field at the ends of the channel decreases slightly. With further development of the streamer channel the number of electrons in it increases more and more slowly and the slope of the distant luminosity isolines begins to decrease (see Fig. 1).

The most detailed data on the development of a streamer in a long discharge gap in neon have been given by Rudenko and Smetanin [1], who observed a shift of the boundaries of the streamer-channel glow. Time dependences of the streamer lengths have been obtained for different values of the external field. A conclusion as to the times at which streamers are initiated at different values of the external field, however, cannot be made on the basis of the results cited. Comparison of the data obtained in this study with the results of [1] is qualitative and is made without relation to the initial time of development (Fig. 4). The calculated curves ($E_0 = 16$ and 8.6 kV/cm in Fig. 4 a and b, respectively) reflect the displacement of fixed level of luminosity at the end of the channel. For the comparison we chose a level of luminosity at which the calculated curves correspond best to the experimental curves $l(x)$ (level 10^{-1} in Fig. 1). According to the data of [1], graphs c and d correspond to $E_0 = 16$ and 8.6 kV/cm, respectively. Curves 1 represent the change in the total length of the streamer and curves 2 and 3 represent the propagation of the cathode and anode streamers, respectively. Qualitative agreement between the experimental and calculated curves is observed at various values of the external field.

Secondary ionization causes a region of weakly ionized gas to form ahead of the streamer channel. The existence of such a pre-ionization zone (PIZ) has an effect on the electron-density profile in the channel. Thus, the profiles of the density n_e in the channel of a streamer developing in a strong external field ($E_0 = 16$ kV/cm) and a weak field ($E_0 = 8.6$ kV/cm)

differ. In both cases rapidly growing PIZs form ahead of the channel up until AST occurs. In the first case, however, in the characteristic streamer travel time $\tau \sim \ell/(v_{st} \pm v_e)$ (ℓ is the characteristic dimension of the PIZ ahead of the channel, v_{st} is the streamer velocity, and v_e is the electron drift velocity) the density of charged particles in the PIZ manages to increase appreciably because of ionization in the external field, since the relation $(v_{st} \pm v_e)/(\alpha_0 E_0 \mu_e \ell) \ll 1$ is satisfied. Here and below the upper sign corresponds to the streamer directed toward the cathode and the lower sign, to the streamer directed toward the anode. Collision ionization thus occurs effectively both in the intensified field directly ahead of the channel and in the external electric field. This is especially pronounced on the cathode side of the channel (see Fig. 3). The channel grows into the PIZ against the background of a uniform increase in electron density along the entire length of that zone. The distributions at the cathode and anode ends of the channel differ. The electron avalanches move with approximately the same drift velocities into the PIZ from different sides of the channel. The avalanche development time in the PIZ is longer on the anode side ($\tau_a \approx \ell/(v_{st} - v_e)$), however, than on the cathode side ($\tau_c \approx \ell/(v_{st} + v_e)$). Secondary avalanches are longer at the anode end of the channel. As a result, the anode front becomes smeared and the streamer moves more uniformly here than in the cathode direction. For $E_0 = 8.6$ kV/cm the coefficient of collision ionization in an external field is fairly small ($(v_{st} \pm v_e)/(\alpha_0 E_0 \mu_e \ell) \geq 1$) and rapid ionization in the PIZ occurs mainly in the intensified field from the streamer-channel side. The difference between the electron-density profiles in the streamer channel from different sides of the channel are smoothed out as the streamer velocity rises, when $v_{st} \gg v_e$.

Calculation shows that the velocity of the anode streamer is higher than the electron velocity in the intensified field at the ends of the channel. Accordingly, the velocity of the anode streamer as well as the velocity of the cathode streamer are determined by the secondary electrons formed ahead of the channel.

The probability of a photon moving a distance R from the channel without being absorbed is $P(R) = \int a_\omega \exp(-k_\omega R) d\omega$ (k_ω is the coefficient of absorption of resonance radiation and a_ω is the spectral radiant density). When $k_0 R_c \ll 1$ (k_0 is the coefficient of absorption of radiation at the center of the line) this probability can be expressed by a simple asymptotic formula. For the collision and Doppler mechanisms of broadening, therefore, we obtain $P(R) \sim (k_0 R)^{-c}$ ($c \geq 0.5$). We assume that the streamer develops in a cylindrical region with an x axis and radius R_c . The propagation of radiation is considered inside a solid angle $\pi R_c^2/R^2$. The probability of absorption of resonance radiation at a distance R from the channel in the given solid angle is

$$D_{av}'(R) = ((4/3) \pi R_c^3 P(R))/R^3 \sim (k_0 R)^{-(c+3)}. \quad (1)$$

It is convenient to assume that the point $R = 0$ is the point of maximum field at the end of the channel. In the coordinate system so chosen the distance R is measured from the point where $E(R = 0) = E_{max}$ along the path of each of the streamers. Accordingly, the density of resonance-excited atoms and the number $N_{esec}(R)$ of electrons formed as a result of associative ionization decrease with increasing R . Finally, only one secondary electron can be formed at a sufficient distance from the channel. The distance at which a single secondary electron is formed, R_{eff} , limits the region of secondary ionization ahead of the stream channel ($N_{esec}(R_{eff}) = 1$). In the calculation the appearance of a secondary electron in a volume V is assumed to be a certain event when $V n_{sec}(R) \geq 1$ (here $n_{sec}(R)$ is the secondary-electron density at a distance R from the channel along the x axis). When $V n_{sec}(R) \leq 1$ the electron creation in the volume V is random and the probability of this process acted satisfactorily in the calculation. The characteristic volume V was assumed to be $(4/3) \pi R_c^3$ and R_{eff} was determined from the x coordinate of the most probable appearance of a single secondary electron. In the region of secondary ionization $N_{esec}(R) \sim P(R)$. The number of electrons in secondary avalanches arrives at the head (at the point $R = 0$) is

$$N_{eh}(R) = N_{esec}(R) \exp \left[\int_0^R (\alpha(r) dr)/(v_{st}/v_e \pm 1) \right]. \quad (2)$$

It can be shown that even though $N_{esec}(R)$ is a decreasing function, $N_e(R)$ increases monotonically as R increases at $v_{st} = \text{const}$. Thus, the most powerful of the avalanches arriving at the head, start at the boundary of the secondary-ionization region. The period

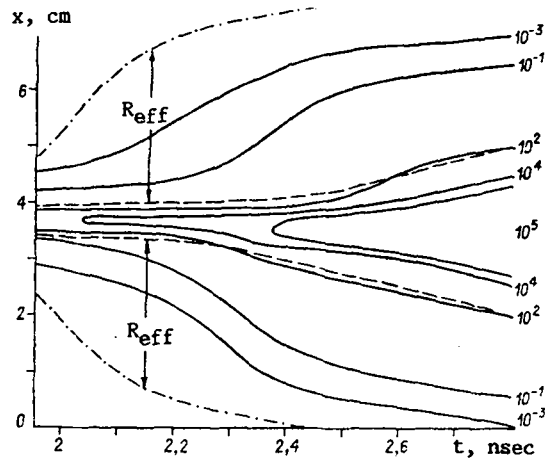


Fig. 5

of rapid change in the number of electrons in the channel in the initial phase of streamer development corresponds to the period of rapid increase in R_{eff} . At the same time, large regions on either side of the channel luminesce uniformly and the PIZs grow. Ionization occurs fairly intensively at the streamer head and directly behind it. The electron density n_{eh} at the head, its luminosity, and R_{eff} and E_{max} as well increase rapidly. As the channel develops, a larger and larger part of it appears in the region of weak field. The growth of the total number of electrons slows down. By the time the motion of the channel accelerates markedly and the derivative $\partial R_{eff}/\partial t$ decreases (see Fig. 1). Despite this, the streamer velocity continues to increase since a fast ionization wave moves along the extended PIZ (Fig. 3). This acceleration phase is the initial phase in the streamer development. A gradual decrease in the derivative $\partial R_{eff}/\partial t$ causes a slight delay in the time to a decrease in the rate at which the streamer velocity grows. The field at the head increases so much that $(\partial\alpha/\partial E)_R \sim R_C \gg (\partial\alpha/\partial E)_R \approx 0$, while directly behind the point of maximum field in the channel the field strength decreases to $E_C < E_0/(2-4)$ at a dimension much smaller than R_C (see Figs. 2 and 3). The dynamics of the streamer motion changes. In fact, the leading part of the channel undergoes phase transfer because of collision ionization in the intensified field. The values of R_{eff} , n_{eh} , E_{max} , and v_{st} remain virtually constant. In this phase of quasisteady development a monotonic dependence of v_{st} on R_{eff} and, therefore, on η_e is established in the leading part of the channel. It is legitimate here to assume an equilibrium situation at the head and in the gap ahead of it. In a coordinate system moving with the velocity of the streamer the distribution of excited atoms is described by the equation $\pm v_{st} \partial n^*/\partial x = n_e/\tau_{ex} - n^*(1/\tau_e + 1/\tau_{ac})$.

Calculations of the streamer for different values of E_0 showed that the electric field in front of the head increases abruptly to $E_{max} \approx (2-4)E_0$ at a distance of the order of the channel radius. When $R > 0$ we have $\alpha(R \sim R_{eff})/\alpha(R \geq R_C) \sim 10^2$ and $\tau_{ex} \ll \tau_{ac}\tau_\ell/(\tau_{ac} + \tau_\ell)$. Behind the head, on the contrary, $\tau_{ex} \gg \tau_{ac}\tau_\ell/(\tau_{ac} + \tau_\ell)$. The density of excited atoms is

$$n^*(r) \approx \frac{n_{eh} R_C}{\langle \tau_{ex} \rangle v_{st}} \exp(-r/R_r). \quad (3)$$

Here the distance r is measured from the head into the channel; $1/\langle \tau_{ex} \rangle$ is the average velocity of collision excitation in the region $R_C \geq R > 0$ and $R_r = v_{st}\tau_{ac}\tau_\ell/(\tau_{ac} + \tau_\ell)$ is the relaxation parameter. For $R_r \sim R_C$ the excited atoms are de-excited mainly in the head. At the secondary-ionization parameters chosen for the calculation such a situation was realized at $E_0 \leq 8$ kV/cm. In fields $E_0 \geq 16$ kV/cm the region of intensive luminescence smears behind the head over a length $R_r \gg R_C$. This dependence of the luminosity distribution in the channel on the experimental field was observed experimentally in [1]. Bearing in mind that $n_{esec}(R_{eff}) (4/3) \pi R_C^3 \approx 1$ and $v_{st}/v_e \gg 1$ as well as (1)-(3), we can obtain for the streamer velocity the equation $v_{st} = S_1(R_{eff}) \ln k_\tau S_2(R_{eff})$, where $k_\tau = (1/\langle \tau_{ex} \rangle) \tau_\ell \tau_{ac} R_C / (\tau_\ell + \tau_{ac})^2 / v_{st}$ is a dimensionless quantity which characterizes the efficiency of the secondary-ionization processes

$$S_1(R_{\text{eff}}) = \int_0^{R_{\text{eff}}} v_e(r') \alpha(r') dr',$$

$$S_2(R_{\text{eff}}) = (1/R_C) \int_0^{\infty} P_{\text{av}}(R_{\text{eff}} + r') \exp(-r'/R_T) dr' \sim$$

$$\sim \int_0^{\infty} [k_0(R_{\text{eff}} + r')]^{-(c+3)} \exp(-r'/R_{\text{av}}) dr'.$$

When the structure of the field in front of the head is taken into account, we can easily show that $R_{\text{eff}} (\partial S_1 / \partial R)_{\text{R}} \sim R_{\text{eff}} \ll S_1(R_{\text{eff}})$. Moreover, from (1) we have $R_{\text{eff}} \sim (n_{\text{eh}} k_{\tau} R_C^c)^{(c+3)} \times k_0^{-c}$. From this we see that the streamer velocity depends weakly on the efficiency of the secondary processes. It is also obvious that the nature of the last dependence is not specific to the quasisteady phase.

The processes in the discharge gap are essentially transient in the electron phase. During the growth of an avalanche in the PIZ there are significant changes in the values of n_{eh} , n^* , R_{eff} , and v_{st} . The dependence of v_{st} on k_{τ} as well as the duration of the stage as a function of the external field strength are difficult to analyze for this stage. From the numerical results it is clear that from the time of the AST the duration of the acceleration phase is of the order of magnitude of $\tau_{\text{acc}} \sim \tau_{\text{AST}} \sim 20 / (\alpha_0 \mu_e E_0)$.

To check the results we carried out a calculation for $E_0 = 16$ kV/cm on a fine, uniform, immobile net with coordinate intervals $h_1 = 0.1 R_C$ and $h_2 = 0.25 R_C$, $\tau = 0.1 \tau_r$. Such calculation requires considerable computer time. The process of streamer development after AST, therefore, was calculated over a short interval of physical time. Enlargement of the net led to poorer resolution of the structure of the field at the maxima. The peak values of the field at the ends of the channel decreased by 35% (as the interval changed from h_1 to h_2). Such a drop in the maximum values of the electric field, however, has little effect on the streamer velocity. The profile of the field ahead of the channel and inside it as well as the streamer velocity varied only slightly ($\lesssim 15\%$).

An indeterminacy exists in the choice of the streamer-channel radius and the parameters responsible for secondary ionization. The value of R_C varied within the limits $\pm 20\%$, causing the characteristic times of streamer-channel development to increase or decrease. The velocity of the streamer in the respective phases varied by no more than 20%. On the whole, however, the qualitative picture of the development remained the same. Variation of the parameters τ_{ac} , τ_{ℓ} , and τ_{ex} by an order of magnitude caused the streamer velocity to change by no more than 50%. On the whole, an increase or decrease by $\pm 100\%$ in any of the parameters responsible for photoionization caused the streamer development time in the acceleration phase to decrease or increase by $\mp 40\%$. The streamer velocity in the quasisteady phase in this case varied by no more than 10%. An order-of-magnitude variation of any of the photoionization parameters led to a corresponding change in the streamer velocity of the last phase by a factor of 1.4-1.7. These results support the conclusion above that the efficiency of secondary ionization has a weak effect on the streamer characterization.

As the streamer channel develops, its conductivity increases, and the time interval necessary for the calculation is reduced. Extension of the streamer calculation to the quasisteady stage of development at given physical parameters requires considerable computer time. A mathematical simulation of a streamer with gas parameters $\tau_{\text{ac}} = 10^{-9}$ sec and $\tau_{\ell} = 10^{-8}$ sec for $E_0 = 40$ kV/cm and $\beta = 2 \cdot 10^{-4}$ cm³/sec. The recombination coefficient β has been artificially overestimated. As a result, the electron density in the channel becomes saturated earlier and at lower values of n_e . The aim of the calculation was to trace the streamer development in the quasisteady state and to demonstrate more graphically the assertions above about the streamer development reaching a quasisteady regime. The pattern of luminosity isolines obtained is shown in Fig. 5. From it we see that R_{eff} decreases slightly by the end of the acceleration phase. In the quasisteady phase the characteristic growth time R_{eff} and v_{st} increase by an order of magnitude in comparison with the corresponding times in the acceleration phase. From this we can easily understand the assumption that the streamer velocity is constant in a long discharge gap (e.g., [3]). Since the characteristic times of variation of the streamer parameters in the quasisteady phase are substantially longer than the secondary-avalanche development times, the dependence of v_{st} on R_{eff} becomes monotonic.

In the initial stage of streamer development the time taken for a secondary avalanche to form ahead of the channel is considerably longer than the characteristic time of variation of R_{eff} , v_{st} , and other parameters of the process. This delay in the development of the streamer channel relative to the appearance of secondary electrons on the discharge axis ($\tau \sim R_{\text{eff}}/v_{\text{st}}$) is disregarded in most a priori streamer models [7, 8, 17]. Such models are suitable for describing a streamer discharge only in very large discharge gaps.

In some gases the cross section for associative ionization is extremely small or this process is absent altogether. In such gases other mechanisms of secondary ionization (e.g., photoionization of various impurities, direct photoionization), which involve excitation of gas atoms and then their deexcitation, operate during streamer development. All of these processes are described by equations of the same form as used in this paper. Since the dependence of the streamer dynamics on the secondary-ionization parameters is weak and their variation does not cause significant changes in the nature of the channel motion, the results of our calculations for neon and, therefore, the conclusions made above can be generalized qualitatively to other gases as well.

LITERATURE CITED

1. N. S. Rudenko and V. I. Smetanin, "Study of the development of streamer breakdown of neon in large gaps," *Zh. Éksp. Teor. Fiz.*, 61, No. 1 (1971).
2. V. A. Davidenko, B. A. Dolgoshein, and S. V. Somov, "Experimental study of the development of streamer breakdown in neon," *Zh. Éksp. Teor. Fiz.*, 55, No. 2 (1968).
3. M. Bayle, P. Bayle, and M. Crokaert, "The development of breakdown in a homogeneous field at overvoltages in helium-neon mixtures and nitrogen," *J. Phys. D*, 8, 2181 (1975).
4. L. E. Kline, "Calculation of discharge initiation in overvolted parallel-plane gaps," *J. Appl. Phys.*, 45, No. 5 (1974).
5. W. Reininghaus, "Calculation of streamers in gaseous discharges," *J. Phys. D*, 6, 1486 (1973).
6. S. K. Dhali and P. F. Williams, "Numerical simulation of streamer propagation in nitrogen at atmospheric pressure," *Phys. Rev.*, 31, No. 2 (1985).
7. É. D. Lozanskii and O. B. Firsov, *Theory of Sparks* [in Russian], Atomizdat, Moscow (1975).
8. G. A. Dawson and W. P. Winn, "Model of streamer propagation," *Z. Phys.*, 183, No. 2 (1965).
9. B. M. Smirnov, *Physics of a Weakly Ionized Gas* [in Russian], Nauka, Moscow (1972).
10. J. M. Geary and G. W. Penney, "Charged-sheath model of cathode-directed streamer propagation," *Phys. Rev.*, 17, No. 4 (1978).
11. I. M. Bortnik, I. I. Kochetov, and K. I. Ul'yanov, "Mathematical model of the avalanche-streamer transition," *Teplofiz. Vys. Temp.*, 20, No. 2 (1982).
12. G. Reter, *Electron Avalanches and Breakdown in Gases* [Russian translation], Mir, Moscow (1968).
13. L. G. Huxley and R. W. Crompton, *The Diffusion and Drift of Electrons in Gases*, Wiley, New York (1974).
14. V. W. Kanl and T. W. Seyfried, "Die Lebensdauer der angeregten Reaktanten in Ventralreaktionen," *Z. Naturforsch.*, 18a, 432 (1963).
15. B. M. Smirnov, *Excited Atoms* [in Russian], Energoizdat, Moscow (1982).
16. V. V. Kremnev, G. A. Mesyats, and Yu. B. Yankelevich, "Development of a single electron avalanche in the nanosecond range," *Izv. Vyssh. Uchebn. Zaved., Fiz.*, No. 2 (1970).
17. A. V. Rodin and A. N. Starostin, "On the theory of cathode-directed streamers," in: *Proceedings of 11th International Conference on Phenomena in Ionized Gases*, Prague (1973).